DIPHOTON AND PHOTON+b/c CROSS SECTIONS AT CDF II

A. BOCCI
(On behalf of the CDF Collaboration)
The Rockefeller University, 1230 York Avenue
New York, NY 10021, USA

A measurement of the rate of prompt diphoton production in $p\bar{p}$ collisions at $\sqrt{s}$=1.96 TeV using the CDF detector is presented. The results are compared to a NLO calculation. We also measured the γ+b and γ+c cross sections comparing the results with PYTHIA LO predictions. The background from non-prompt sources is estimated using a statistical method based on differences in electromagnetic showers initiated by photons and by the background.

1 Diphoton Cross Section

The production of prompt photon pairs is one of the cleanest signatures at a hadron collider providing a precision test of many aspects of Perturbative Quantum Chromodinamics (pQCD). On one side, final state photons can be measured experimentally with extreme accuracy thanks to the excellent resolution of Electromagnetic calorimeters. On the other side, by emerging directly from the parton hard collision, they are free from all the theoretical complications carried by the hadronisation process of quarks and gluons. A large amount of prompt diphoton data have been collected during the Run II by the CDF experiment offering the opportunity to test our understanding of this process. A preliminary comparison [3] of these data to the prediction of the diphoton production rate and kinematic distributions have been performed. Furthermore, the same final state serves as a signature of many new physics searches, like the presence of large extra dimensions or heavy new particles predicted to have two photons in their cascade decays. Finally, the $\gamma\gamma$ production with large invariant mass is a *irreducible* background for a light Higgs boson search in the two photon decay channel at the forthcoming LHC. This background is huge and needs to be precisely evaluated.

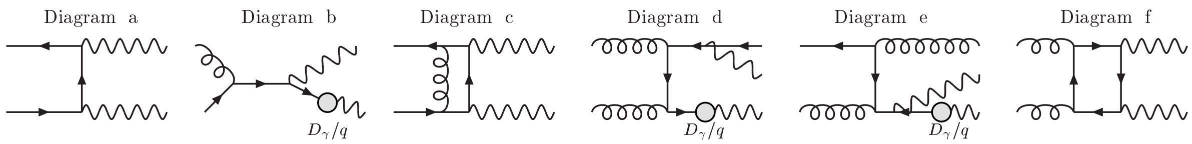

Figure 1: Some subprocesses for diphoton production at the Tevatron. There are sketched examples of LO (a, b) and NLO contributions (c, d, e) produced either through a direct (a, c) and a fragmentation mechanism (b, d, e). A subprocess (f) initiated by gluons (technically at NNLO) is also pictured.

1.1 Production Mechanism

The subprocesses for diphoton production are typically divided in two categories: (1) the direct mechanism, when they take part directly on the hard process, and (2) the fragmentation mechanism, when one (or both) photons result from the fragmentation of high P_T quarks or gluons[a]. The leading order (LO) subprocesses for diphoton production at the Tevatron are of order α_{em}^2. They include both direct and fragmentation diagrams (see (a) and (b) in fig. 1). At the next-to-leading order (NLO) there are several subprocesses contributing to diphoton production (see (c,d,e) in fig. 1). The NLO contributions allow more initial states and extra particles in the final state influencing observables sensitive to kinematical configurations forbidden at leading order; an important example occurs when the direction of the two photons are close to each other (see (f) in fig. 1), a process that is enhanced by the fragmentation mechanism. At hadron colliders, the huge background by neutral meson decays produced in the fragmentation of quarks and gluons compels tight isolation cuts in the identification of prompt photons. Therefore photons from fragmentation are also rejected making impossible an inclusive measurement. Nevertheless the isolation cuts applied at CDF (see par. 1.2) do not remove completely the contribution from single fragmentation processes, although totally suppress the double fragmentation. Three different Monte Carlo programs were used to compare the theoretical predictions to the data[1]: (1) DIPHOX, a full NLO QCD calculation[b]; (2) ResBos, a LO calculation with $q\bar{q} \to \gamma\gamma$ subprocess at NLO and including soft initial gluon radiation resummation effects, (3) PYTHIA, a LO order calculation parton shower Monte Carlo.

1.2 Photon Identification

To identify photons we look for collimated clusters of energy in the electromagnetic calorimeter with very low activity in the hadronic compartment and with no tracks pointing into it. To reduce the hadron contamination (jets) we reject (isolation cut) all the events with an extra energy greater than 1 GeV in a cone of radius 0.4 (in $\eta - \phi$ space) around the photon. We require also the shower profile to be compatible with that one of a single electron as measured in the test beam. Finally we perform a statistical subtraction to get rid of the multiple photon background. It exploits the difference in the shower profile between signal and background and the different conversion probability of single and multiple photons[3].

1.3 Outline of the analysis

This analysis [1] uses the data collected between February 2002 and September 2003, corresponding to an integrated luminosity of 207 pb^{-1}. The events have been filtered by a diphoton trigger

[a]The singularities appearing from the "collinear enhancement" parton splitting are factorized and absorbed into a gluon (or quark) fragmentation functions to a photon $D_{\gamma/g}(\hat{z}, M_f^2)$, where M_f is an arbitrary fragmentation scale. This gives rise to some ambiguity in distinguish the two mechanisms and thereby one should always bear in mind that only the sum of the two is meaningful.

[b]Now also including NLO corrections for $gg \to \gamma\gamma$ (technically beyond NLO for the $p\bar{p} \to \gamma\gamma$ process) important in some kinematical region where the gluon parton distribution in the proton is high

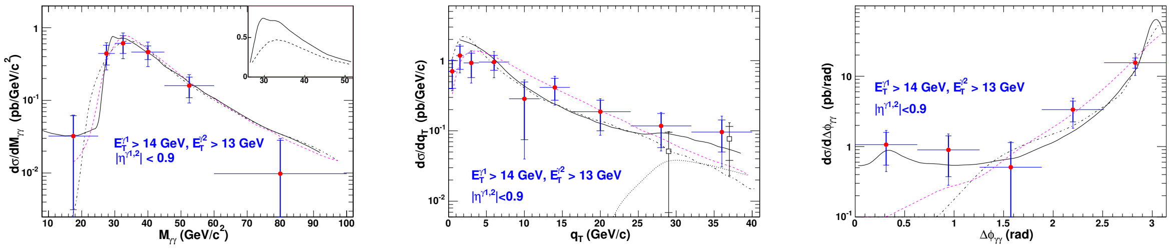

Figure 2: CDF Run II data compared with predictions from DIPHOX (solid), ResBos(dashed) and PYTHIA(dot-dashed). The PYTHIA predictions have been scaled by a factor 2. Both statistical only (innermost notch), and statistical and systematic errors combined are shown. The first plot shows the $\gamma\gamma$ mass distribution and, in the inset, the DIPHOX NLO cross section with/without (solid/dashed) the gg contributions. The second plot shows the q_T distribution and, at high q_T, the DIPHOX (dot) and CDF data (open squares) contributions from the configuration where the two photons have $\Delta\phi < \pi/2$. The third plot shows the $\Delta\phi$ angle distribution.

requiring two EM clusters with $E_T > 12$ GeV. The offline cuts require the presence of a photon (as described in sec 1.2) with $E_T > 14$ GeV and another photon with $E_T > 13$ GeV. Only photons falling in the fiducial region of the central calorimeter ($|\eta| < 0.9$) are selected. The total efficiency is $\epsilon_{tot} = 0.152$ and the number of diphoton events after all the cuts are $N_{\gamma\gamma} = 427 \pm 59$ $(stat)$.

1.4 Data-Theory Comparison

From the final selected sample we extracted the differential cross section with respect to some kinematic variables X as:

$$\frac{d\sigma}{dX} = \frac{\Delta N_{\gamma\gamma}}{(L \times \Delta X \times \epsilon_{tot})} \tag{1}$$

and we compared them with the theoretical prediction. $\Delta N_{\gamma\gamma}$ is the number of events in a bin of size ΔX and L the integrated luminosity. The results for three kinematical variables - $m_{\gamma\gamma}$, q_T [c] and $\Delta\phi$ - are shown in fig. 2. Since the background can vary with the kinematics, it is calculated bin by bin. This results in a higher statistical error but reduces systematics.
Some comments about these results:

- $m_{\gamma\gamma}$ *distribution*: Data agree pretty well with the predictions and in the lowest bin, where the contribution of NLO dominates (see for example the diagram (e) on fig. 1), they seem to prefer DIPHOX. The inset also shows that the $gg \to \gamma\gamma$ subprocess is quite relevant in the low dijet mass region, although it is a NNLO contribution.

- q_T *distribution*: For $q_T \to 0$ NLO calculations became unstable because of the presence of singularities. ResBos behaves better than DIPHOX thanks to the resummation on soft initial gluon radiation. At high q_T DIPHOX presents a shoulder brought about by more space phase accessible only at NLO. ResBos, lacking a full NLO calculation, does not predict it. In the same plot the q_T distribution is shown for those events with $\Delta\phi < \pi/2$, a "NLO-only" space phase region responsible for the shoulder at ≈ 30 GeV.

- $\Delta\phi$ *distribution*: In this plot is even more evident the enhancement caused by the NLO contributions at low $\Delta\phi$. Moreover the raise at very low $\Delta\phi$ is caused by the diverging fragmentation part (collinearity) reduced by the isolation cut at $\Delta R < 0.4$. At high $\Delta\phi$ instead the resummation is again important and DIPHOX predictions become unstable.

[c] It is the module of the transverse momentum of the $\gamma\gamma$ system: $\vec{q}_T = \vec{P}_T^{\gamma_1} + \vec{P}_T^{\gamma_1}$

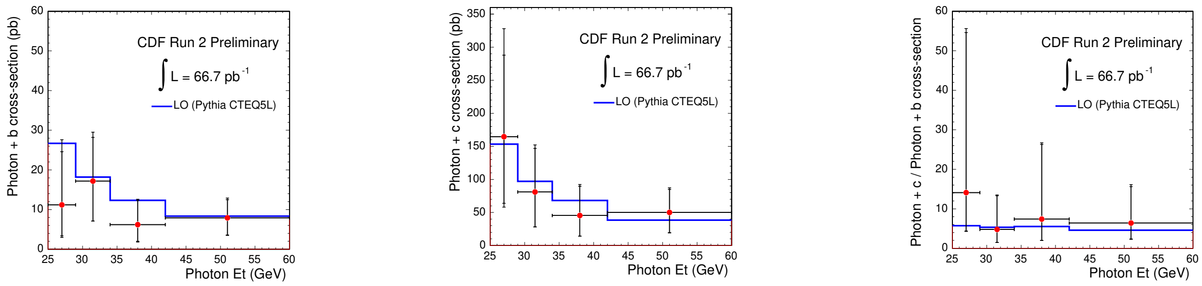

Figure 3: The three plots are respectively the $\gamma + b$ cross section, the $\gamma + c$ cross section and the ratio of the two as a function of the photon E_T. In all cases the data are shown by points and LO expectations by the solid line. Both statistical only (innermost notch), and statistical and systematic errors combined are shown.

In conclusion, with the present statistical and systematic errors there is an overall agreement between data and theoretical predictions. With more data coming in the present Run II, a better comparison will be soon available.

2 Photon+b/c Cross Section

The production of an isolated photon in association to a heavy flavor jet is of a great interest for testing the QCD theory. Some extensions of the Standard Model predict an enhancement of the γ+b/c cross sections through light stop or Technicolor production [4]. Using Run II data CDF measured the γ+b and γ+c cross sections. The dataset used in this analysis corresponds to an integrated luminosity of $66.7 \pm 3.8 \ \ pb^{-1}$. Candidate events have been selected using a high P_T photon trigger and offline cuts require the presence of a photon (as described in sec 1.2) with $E_T > 25$ GeV. At least one jet with $E_T > 30$ GeV is required. These cuts result in an acceptance $\epsilon_{sel} = 0.242$. In order to select events with a heavy flavor jet, only events with a secondary vertex more than two standard deviations away from the primary vertex ("*tagged*" events) were selected. The tagging efficiency is typically 25% for b-jet and 4-5% for c-tag. Using the Monte Carlo, secondary vertex mass distribution templates for b, c and light quarks are built and the same distribution for the data is fitted to a combination of these templates. The outcome gives the flavor composition for the data sample. The total number of events with a real photon and a tagged jet is 770 ± 99 which 161 ± 77 are γ+b and 340 ± 107 are γ+c. The cross section is calculated dividing the number of events by the integrated luminosity and the total efficiency. The results are plotted as a function of photon E_T in fig. 3. The total cross section is $40.6 \pm 19.5^{+7.4}_{-7.8}$ pb for the $\gamma + b$ and $486.2 \pm 152.9^{+86.5}_{-90.9}$ pb for the $\gamma + c$. The main source of uncertainties arise from the jet energy scale and the photon background subtraction. For the $\gamma + c$ the c tag efficiency is also relevant. Calculating the ratio of the two cross sections most of the uncertainties cancel out and the results are plotted in fig 3. The total cross section ratio is $6.4^{+9.2}_{-4.0}$. With the present data no deviation from the Standard Model predictions is observed.

References

1. Yanwen Liu, PhD thesis, University of Geneva, 2004;
   CDF Collaboration, submitted to PRL
2. T. Binoth *et al*, *Eur. Phys. J.* C **16**, 311 (2000);
   C. Balazs *et al*, *Phys. Rev.* D **57**, 6934 (1998)
3. F. Abe *et al*, *Phys. Rev. Lett.* **70**, 2232 (1993).
4. F. Abe *et al*, *Phys. Rev. Lett.* **83**, 3124 (1999);
   T. Affolder *et al*, *Phys. Rev.* D **65**, 052006 (2002);